Electromechanical Energy Conversion Systems (EECS)
Niroo Research Institute (NRI)
Vol. 2, No. 2, Summer 2023, 7-15
DOI: 10.30503/EECS.2023.404121.1041
Original Article

Electric Drive Command for Green Resource Adopting AC Microgrids

Eman M. Abdzaid [1], Ali Abdul Razzaq Altahir [*1], Ahmed Zurfi[1], Uday A. Alhamdany[1]

Abstract

An electric drive controller for AC microgrids with renewable energy sources is a system that controls the flow of electricity in an alternating current (AC) microgrid, which is powered by green resources such as PV solar and wind power. The role of distributed generation in the electricity industry has been expanding in recent years. Distributed (DGs) are small, scalable units, generally with a capacity of less than 10 MW which can be connected to the grid, distribution feeders or customer levels. Nowadays, the high penetration of distributed resources in power systems is increasing. Since these units can play an important role in electricity markets and provide ancillary services for system operators, integrating these resources within power systems has been considered. Therefore, this paper focuses on modelling, designing and simulating a suitable controller to ensure AC microgrids stability and stable performance (AC MG) in both grid-connected and islanded modes. Meanwhile, all simulations have been fulfilled in the MATLAB environment. After designing the controllers and ensuring the performance of their frequency response using the bode diagram and the system step response, these controllers were used to command the voltage and current in real scenarios. After applying the controllers, the performance has dramatically improved in the voltage and current controller presence. As a result, the controller can be programmed to respond to changes in the energy supply and demand, adjusting the output of the green resources and managing energy storage systems within the microgrid. This allows the system to operate stably and sustainably, even when there are fluctuations in the energy supply or demand.

Keywords: Control of distributed generators, electric drive controllers, photovoltaic systems and wind turbines.

Received Date: 2023-06-26; Revised Date: 2023-07-02; Accepted Date: 2023-08-08

1. INTRODUCTION

The electric drive controller is accountable for managing the V/Hz of the AC power supply, as well as controlling the speed of electric motors and generators within the microgrid. This ensures that the system operates efficiently and reliably and that the renewable energy resources (RER) are used to their maximum potential. Conventional power plants to generate electricity have grown and developed. These power plants, mainly thermal, use fossil fuels to produce electrical energy. Low efficiency, high heat production, and burning of fossil fuels have increased the necessity of optimal use of these fuels and the tendency to produce electric power based on new energy sources. In recent years, many solar and wind power plants have been designed and installed on both small and large scales. The development of approaches to using distributed generation resources, energy storage systems (E.S), and smart grids has created higher performance and much more complex systems. In addition, the high penetration of generation resources distributed in the network caused problems such as voltage and frequency stability, control and coordination between power generation units. With the growth of electronic energy-based devices and progress in storage systems, a new structure for electrical energy generation systems, “Microgrids” [1], has emerged. Microgrids (MGs) are small networks consisting of several distributed generation sources and batteries, which can be A.C, DC or hybrid. Moreover, MG can operate in parallel with the main network or offline (or island) [2]. In the island-based mode of operation, MGs are responsible for transmitting and supplying power to their local loads.

In addition, as mentioned earlier, the main power plants are based on A.C systems. A.C. microgrids are also more popular. It should be noted that compared to A.C systems, the protection of D.C systems is much more complex than A.C one and they need the construction of a special foundation, but the major drawbacks of A.C. MG.s are reactive power and the need to synchronise them with the grid [3]. A.C. MG.s generally include some loads, transmission lines and DGs. Unlike wind generation systems, the output power of solar systems is

[1] *Electrical and Electronic Engineering Department, University of Kerbala*, Iraq
**Corresponding author, Email:* ali.altahir@uokerbala.edu.iq

D.C; therefore, dc/dc power electronic converters are responsible for converting power from D.C to A.C [3]. Because of the existence of these conversion classes, the control becomes more complex, which lowers the system's effectiveness and dependability. Power electronic converters play a crucial role in managing MGs [4]. The main idea is to design a stable controller that can enhance the performance of the DC drive. The controller can be programmed to react to any change in source or demand, modifying the output of the sustainable resources and managing energy storage systems within the microgrid.

The summary of the current research is: section 2 presents renewables sources and microgrids, section 3 discusses control of microgrids, whilst section 4 talks about AC microgrid modes of operation, then section 5 states the implementation of the proposed system and after that implementation of the proposed system is simulated. Finally, the conclusion has been drawn in section 6.

2. RENEWABLE SOURCES AND MICROGRID

Microgrids can reduce costs, such as the construction of transmission lines, as much as possible due to proximity to the load. Usually, DGs, whether clean or non-clean, are connected through the common DC bus. Power Electronic converters are commonly used to connect them to the grid [19].

The converters used in MGs can be grid feeders or support the grid. When utilized as a feeder source, the first class of converters have high parallel impedances and can inject both real and imaginary power into grids next to them. The grid itself or the second category of converters determines the amplitude and frequency of the output voltage in the voltage source converter. Grid-backup converters can function in both network-connected and islanded modes of operation. Solar and wind power-based sources are the only uncontrolled and distributed generation (DG) types that are consistently found in microgrids. Controllable DGs such as diesel generators with the ability to produce flexible and controllable power are essential equipment based on A.C in microgrids. Because microgrids are converter-based systems, they Sub partition every individual section number as follows. have low inertia, so a sudden disruption between production and consumption can be detected and compensated by an energy storage system in the islanded mode. Controllable D.G.s such as diesel generators with the ability to produce flexible and controllable power are essential equipment based on A.C in microgrids. Because microgrids are converter-based systems, they have low inertia, so a sudden disruption between production and consumption can be detected and compensated by an energy storage system in the islanded mode. Two important sources of renewables are solar and wind, which will be discussed as follows.

2.1 Solar Panels Generation System

Solar panels (or photovoltaic systems) include several solar cells in the form of series and parallel structures. These cells provide electricity by absorbing solar radiation and translating it into electricity. An electrical model is commonly used to check the performance and features of solar systems. Two well-known electrical models for examining the performance of solar panels under different temperature and irradiance conditions are the lone and dual diode models [4].

PVs' output voltage is DC, and therefore inverters either three phases or single phase are used to connect them to the grid. The two parameters affecting the performance of solar panels are temperature and radiation. With the reduction in radiation, the panel's ability to absorb photon energy will have reduced subsequently. Moreover, temperature also hurts maximum power absorption.

Solar panels can be classified into a variety of crystalline, multi-crystalline and amorphous types according to the type of silicon used.

2.2 Wind Turbine Generation System

The electrical schematic of a doubly fed induction generator or DFIG. This structure usually has advantages such as the depreciation of fewer mechanical devices, the ability to control mechanical speed and maximized power absorption from the wind turbine.

The wounded rotor generator's stator is linked to the network, and the induction generator's rotor is similarly connected to the network via two back-to-back power electronic converters. To explore the qualities and how the DFIG system functions, each turbine component with the generator should be represented [5].

3. CONTROL OF MICROGRIDS

Along with the many benefits of small grids, there are also several disadvantages and problems associated with MGs. Heavy load changes and fault occurrence (single, two and three-phase faults) cause voltage and frequency fluctuations in MG.s, and due to lack of support in the islanded mode, they are prone to voltage fluctuations which may lead to instability and ultimately the collapse of the MG. [5, 6]. Therefore, the MG control problem is essential because the inertia of D.G.s is very low.

To maintain the stability and coordination of existing units within the MG., there is always a need for a control strategy to ensure stability and proper power

sharing. In MG, whether A.C. or D.C., power electronic converters (dc/dc converters or inverters) are responsible for controlling vital parameters such as frequency and voltage [1]. The microgrid control system must be reliable in case of reference changes or load changes, maintaining the overall system's stability so that it does not collapse. Generally speaking, the control system is responsible for balancing D.G.s and loads, controlling the current and voltage of the microgrid to track predefined trajectories and guarantee the economic load distribution.

The complexities of MG.s' control, despite the high penetration of D.G.s, depend on their connection type [1]. The distribution network acts as the main bus to balance power in network-connected mode. In this case, the inverter should be able to optimally control the voltage and current in the MG.

If the MG. enters the islanded mode or is isolated from the grid, the inverter acts as a voltage source to keep V/Hz within the permissible limits.

The most important control variables in MGs are voltage, frequency, and reactive power. Therefore, the MG controller has the following responsibilities:

• Adjust voltage and frequency under working conditions

•Transients from network-connected mode to grid-disconnected mode and vice versa.

• Real and imaginary power control for proper power sharing in the condition connected to the network and disconnected from the grid

• Participation in the energy market while producing micro sources at their best

• Continuous power supply for critical services including hospitals, schools, and other sensitive loads

• Optimization of production cost and load exchange with adjacent network. To have stable and reliable performance in MG.s with several D.G.s, having energy management strategies (EMS) is essential. EMS, by assigning real and imaginary power at the setting point to D.G units, provides the conditions of a suitable and economic power-sharing along with keeping the balance of production and load, placing the frequency of the system with a rapid response when disturbances and transients occur, and thus creating a non-autonomous condition in the grid-connected state [7].

3.1. Hierarchical Control of Microgrids

This control strategy consists of three primary, secondary and tertiary stages with specific objectives at each level [8]. The primary level of control is carried out by the local controller in the interface converter terminals. The primary attraction of this level is the precise real and imaginary power-sharing control among D.G. units achieved by combining power controllers and controlling the voltage amplitude and frequency of VSC terminals. Therefore, this level of control provides voltage and current along with power coordination in the centralized and decentralized form. Due to the rapid dynamics of the primary control among other control layers, it includes power sharing and voltage control [9]. Both linear and nonlinear designs are possible for the controller used for active power control. The linear controller may be composed of a proportional-integral (P.I.) controller with simultaneous rotation of the reference frame capability, state feedback, an adaptive controller with fixed reference resonance, model predictive control, and dead bit. [10]. The primary level of control is to regulate crucial MG parameters like voltage and current.

3.2. LC Filter Design

Since switching frequency and voltage distortion can lead to undesirable power quality, designing a suitable filter can compensate for the undesirable effect of the aforementioned phenomena. Due to the existence of an inductor and a capacitor, the filter would be second-order. Therefore, as mentioned in reference [11], these types of filters provide a -40 dB per cycle phase margin for compensation.

Generally speaking, it can be stated that the presence of inverters in systems based on D.G.s (or inverter-based D.G systems) is necessary to achieve low distortion and optimal power quality.

3.3. Output Inductor Design

The capacitor is connected as parallel with an inductor. The resonance frequency in this filter is calculated by using the following equation:

$$f_o = \frac{1}{2\pi}\frac{1}{\sqrt{LC}} \quad (1)$$

In the equation above, L is the inductor, and C is the capacitor. The inductor determines the desired current ripple and compensates for the low-frequency harmonics. The current must first be calculated to calculate the amount of inductor in the filter. To determine an equation to calculate the amount of L, consider the following equation:

$$V_L = V_{Ia} - V_{ga} \quad (2)$$

In (2), the voltage V_{ga} is the phase voltage of the network and the V_{Ia} is the phase voltage of the inverter. To calculate the maximum rate of current ripple, one can obtain the followings:

$$\begin{aligned} V_{Ia} &= \frac{2}{3}V_{rms} \\ V_{ga} &= \frac{1}{2}V_{rms} \\ V_L &= \frac{1}{6}V_{rms} \end{aligned} \quad (3)$$

According to harmonic standards, the acceptable range for harmonic content is typically between 15-20% of the nominal current. Therefore, assuming 20% harmonic content, the maximum amount of current ripple will be under the following relationship. As described in the following equation, the ripple current depends on the frequency of switching, D.C. bus voltage or inverter (Vrms) voltage and inductance [11].

$$V_L = L\frac{\Delta I_L}{\Delta T_s}, \quad \Delta I_L = \Delta T_s \frac{V_L}{L} \tag{4}$$

By substituting the V_L from equation (4) in equation (5), it can be written:

$$\Delta I_L = \Delta T_s \frac{V_L}{L} = \Delta T_s \frac{1}{6L} V_{rms} \tag{5}$$

Finally, assuming that the working cycle of a phase voltage in the maximum output is equal to 75%, therefore, equation (7) can be written as:

$$\Delta I_L = \frac{1}{8Lf_s} V_{rms} \tag{6}$$

And the output filter will be as follows:

$$\Delta I_L = \frac{1}{8Lf_s} V_{rms} \tag{7}$$

3.4. Output Capacitor Design

Likewise, one can obtain an equation for the capacitor. Suppose that ω_{res} is the resonance frequency:

$$C = \frac{1}{L{\omega_{res}}^2} \tag{8}$$

In capacitor design, it is assumed that the maximum power factor changes seen in the grid would be 5% [12].

4. AC MICROGRID MODES OF OPERATION

Due to the operating conditions of MGs, they can operate in both modes.

4.1. Network Connected Mode

In network-connected mode, the MG. injects power into the network. The dynamic behaviour, in this case, is also determined based on the grid itself.

The circuit equivalent to the inverter with the controller is shown in Fig. 1.

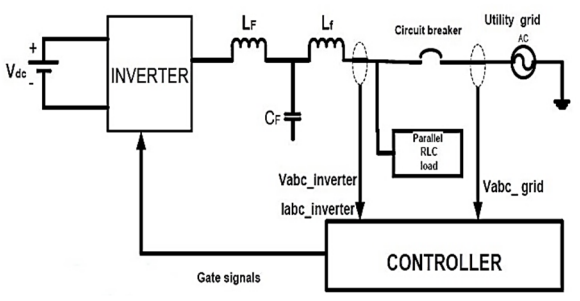

Fig. 1. A TYPICAL AC MG. IN CONNECTED MODE [13]

4.2. Islanded Mode

In islanded mode, MGs are responsible for supplying their local loads. As depicted in Fig. 2, this operating mode is detected as a result of a fault by the protection devices, i.e. relays, and is associated with the opened grid-connected key. As mentioned above, in this case, in addition to supplying its load power, the MG. performs the task of adjusting and stabilizing the frequency and voltage to maintain the stability of the whole system.

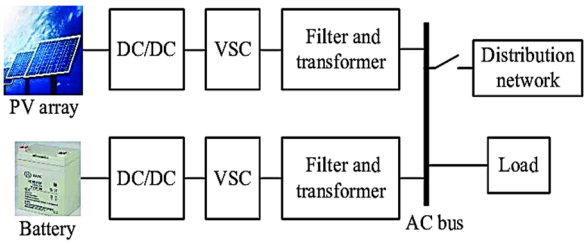

Fig. 2. A TYPICAL AC MG. IN ISLANDED MODE [6]

In this mode, inverters perform the majority of the control work, while droop, the most well-known control technique, is in charge of distributing power among the resources.

In the following, the modelling and design of voltage and current controllers in two operational modes and then the power-sharing algorithm based on the droop method will be mentioned.

4.3. Modelling in Grid-Connected Mode

Table 1 shows all the information regarding the simulation of two single-layer wound stator magnetic gears. The function of these two gearboxes is analyzed and compared using the FEM method. To fairly compare the conventional gear and the proposed gear, structural information in both gearboxes is considered identical.

To model the diagram block, suppose the circuit model of the whole system is given in Fig. 3.

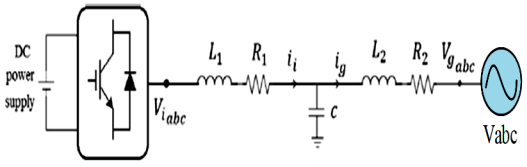

Fig. 3. INVERTER-BASED DG WITH LC FILTER [13]

As mentioned earlier, the voltage grid is stabilized by the grid. Therefore, the control goal is merely to control the current in the MG. To design the controller, as shown in Fig. 4, the tracking error value is obtained by taking feedback from the inverter component and comparing it with a reference value.

Then this error value enters the current controller and is multiplied in an output gain. After comparing it with a reference value, the output voltage of the inverter is finally entered into the L.C. filter. It is assumed that the grid has harmonic content, and therefore the resonant current controller is selected and designed to compensate for the harmonics in the signals.

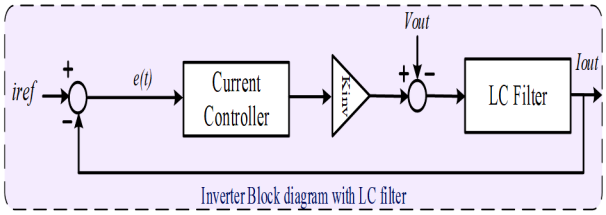

Fig. 4. CURRENT CONTROLLER MODEL: SINGLE-LOOP [13]

The block diagram of the LC filter is given in Fig. 4, and controller transfer functions are as follows [13]. The r_L value is a small series resistance. By implementing the Mason principle, the system's closed-loop transfer function can be written with the following equation:

$$G_{ref-iout} = \frac{\frac{1}{Ls+r_L}}{1+(\frac{1}{Ls+r_L})(K_P+\frac{K_I\, s}{s^2+2\omega_c s+{\omega_0}^2})} \quad (9)$$

Similarly, the diagram block model of the system can be extracted in the islanded mode.

5. IMPLEMENTATION OF THE PROPOSED SYSTEM

The previous steps were the first step in designing voltage and current controllers in MG.s. After ensuring the accuracy of the designed controllers in both operating modes and applying various scenarios such as external disturbances, voltage-current reference changes, and sudden load changes, the system response will be evaluated. If the obtained solutions were desirable, then,

$$C\ Filter = \frac{1}{Ls+r_L} \quad (10)$$

$$R\ Controller = K_P + \frac{K_I\, s}{s^2+2\omega_c s+{\omega_0}^2} \quad (11)$$

in the second step, the droop control strategy is applied to the designed MG.s to ensure appropriate power sharing between units. In Fig. 5, the whole system structure of connection is given in Fig. 5.

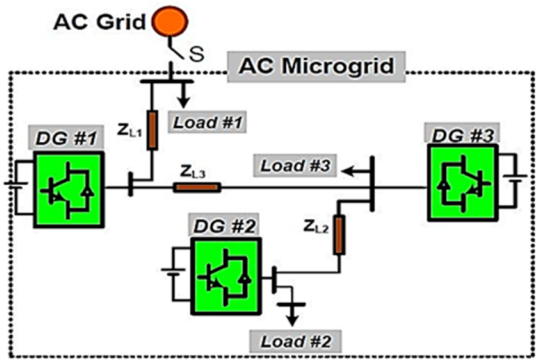

Fig. 5. HOW D.G.S ARE LOCATED IN AC MG

In actuality, the goal of the grid-connected mode was to regulate load current. The voltage of MG. is intended, nonetheless, in the islanded mode. Therefore, in this case, a power-sharing algorithm is necessary to maintain the system's stability. The most commonly used control method in this case for MG is voltage and frequency droop [14]. As can be seen in Fig. 6, the MG comprises three DG units, transmission lines and some local loads. Each DG unit is equipped with a voltage control system designed in the first step (using a multi-loop controller).

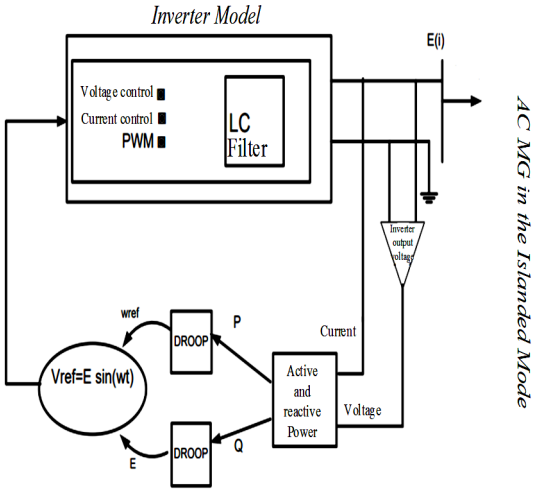

Fig. 6. THE CONTROL DIAGRAM OF AC MG [43]

5.1. Design and calculate the LC filter

In the first step, simulation requires that the parameters of the inverter and the number of filters be determined. The inverter has three-phase. Since the output voltage of the inverter has harmonic contents, it is required to design a filter to remove them. The amount of inductor L is determined according to the current ripple. The MG.'s parameters are given in Table 1. The amount of capacitor C is calculated according to the criteria discussed in the previous chapter. The internal resistance of inductors and capacitors is also assumed that the inverter efficiency

is very high (about 98%) and only one percent of losses per phase exists.

Table 1. A.C. MICROGRID SPECIFICATIONS FOR SIMULATION

AC MG. voltage (V_{rms})	700 V (three-phase rms)
D.C. bus voltage	400V
MG. voltage variation	$\pm 10\%$
Grid frequency (f_{grid})	50Hz
Switching frequency (f_{sw})	10KHz
Grid harmonic component	THD=2% (3,5,7,,11,13)
Inductor current ripple(ΔI_m)	4% in nominal power
Nominal power (P_{inv})	4kW
Base power (Sbase)	60 kVA
Grid impedance	Z= 0.6+0.2j

Considering the parameters given in Table 1, the amount of inductor and capacitor can be calculated as follows:

$$f_{res} = 0.05 f_{sw} = 500Hz,$$

$$\omega_{res} = 2\pi f_{res} = 3.141\ KHz$$

$$I_m = \sqrt{\frac{2}{3}\frac{P_{inv}}{V_{rms}}} = 8.16\ A$$

$$\Delta I_m = 0.04 I_m = 0.326$$

$$L = \frac{V_{rms}}{8 f_{sw} \Delta I_m} = 26.88mH$$

$$C = \frac{1}{L\omega_{res}{}^2} = 3.781\mu F$$

$$P_{loss} = 40Watt$$

$$I_{rms} = 5.77A$$

$$r_L = r_C = \frac{P_{loss}}{3 I_{rms}{}^2} = 0.4\Omega$$

$$S_{base} = 15 \times P_{inv} = 15 \times 4KVA = 60kVA$$

$$Z_{base} = \frac{V_{rms}{}^2}{S_{base}} = 0.4\Omega$$

$$Z_{grid} = \frac{0.6 + j0.2}{100}\ pu = \ 0.000016 + j0.000005\ \Omega$$

5.2. Inverter Block Diagram Simulation

5.2.1. Connected Mode and Current Controller

In the network-connected mode, without the controller, the inverter diagram block model will be under Fig. 7.

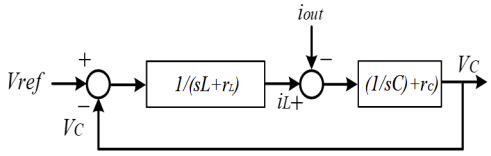

Fig. 7. INVERTER BLOCK DIAGRAM MODEL IN A GRID-CONNECTED MODE WITHOUT CONTROLLER

If one wants to draw the output voltage transfer function to the inverter input by applying the Mason rule, the transfer function of the closed-loop system can be written. The SISO tool or linear control analysis can be used in MATLAB software to apply the controller for such a transfer function. For instance, a bode diagram considering the calculated inductor and capacitor values is shown in Fig. 9.

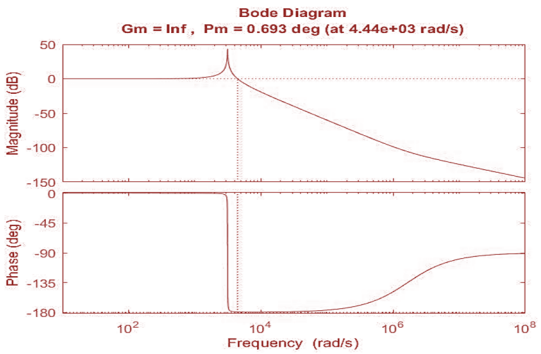

Fig. 8. PHASE MARGIN DIAGRAM AND SYSTEM GAIN WITHOUT CONTROLLER

Figure 8 shows the diagram of the closed loop. The transfer function of output voltage to input (Vout/Vin). Using this diagram, information can be obtained about system stability, phase and gain margin as the system's step response.

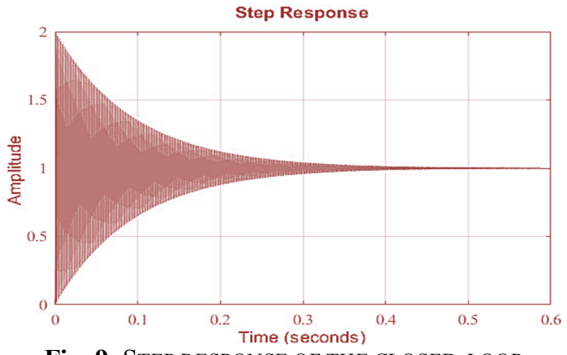

Fig. 9. STEP RESPONSE OF THE CLOSED-LOOP TRANSFER FUNCTION

As shown in Fig. 9, the step response is not desirable without a controller. In other words, the amount of phase margin and gain at the given frequency is insignificant. Therefore, this amount should be modified and selected using a voltage or current controller so that the system response becomes desirable. In this regard, the system transfer function is defined first by using the SISO tool in MATLAB software. In addition, the designs will be carried out in two modes: single-loop controller and multi (or double) loop, as mentioned in the previous chapter. As an example, assume that the variable under the controller is the output current, then we would have:

$$T\_i_L\_i_{ref} = \frac{\left(\frac{1}{R_L+SL}\right)}{1+\left(\left(\frac{1}{R_L+SL}\right)\times\left(R_f+\frac{1}{SC}\right)\right)} \quad (12)$$

$$T_{out} = \frac{Y_{out}}{1+T\_i_L\_i_{ref}\times T_{Cont}} \quad (13)$$

By extracting the transfer function $T\_i_L\_i_{ref}$ using the SISO tool allows modification of the phase margin and the controller gain by adding zero and pole to the transfer function. Adding zeros and poles will be continued until the desired phase margin is obtained. Notably, a general rule of thumb is that the desired step response should be done in the switching frequency range. By doing that, the current controller was designed, and its transfer function was extracted and applied to the system. The following figures illustrate the phase and gain margin diagrams with the system's step response.

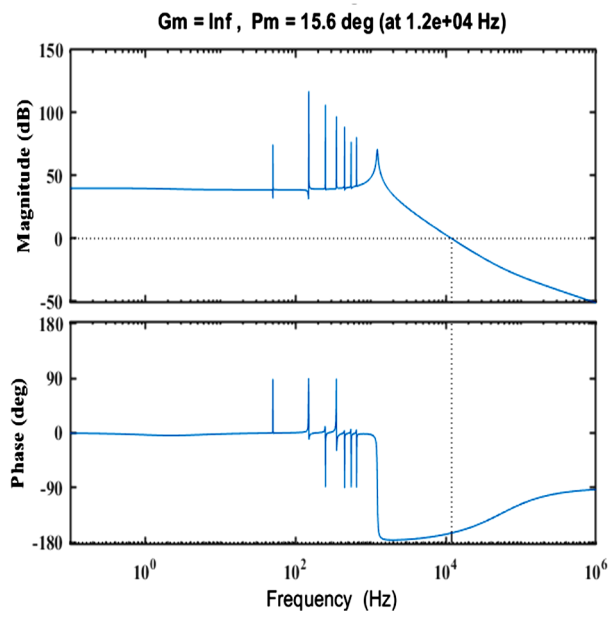

Fig. 10. BODE GRAPHIC OF THE CURRENT CONTROLLER-CONSIDERED CLOSED-LOOP TRANSFER FUNCTION

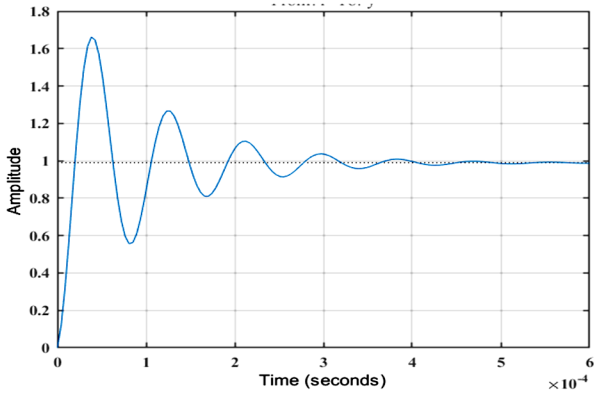

Fig. 11. THE STEP RESPONSE OF THE SYSTEM IN THE PRESENCE OF THE CONTROLLER

According to Figs. 10 and 11, after designing the controller, it can be seen that the system's step response has been dramatically improved to a desirable extent. In addition, the phase margin of the system is suitable around the switching frequency. According to Fig. 11, it can be seen that the system has converged to its final value in a short time after a brief period.

It should be noted that the designed controller is not unique it is possible to change the transform function of the controller by tuning the controller coefficients and moving zeros and poles. In other words, there is countless transfer function for controller design. Now, after ensuring the controller's performance and exporting the obtained transfer functions to the Simulink environment, the controller's performance can be evaluated in real simulation. In grid-connected mode, the following scenarios are considered to evaluate the performance of the MG. under study:

5.2.2. Islanded Mode and Voltage Controller

The islanded mode's multi-loop controller block diagram is given in Fig. 12.

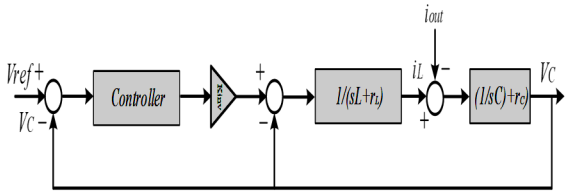

Fig. 12. VOLTAGE CONTROLLER DIAGRAM BLOCK (MULTI-LOOP BLOCK DIAGRAM) IN ISLANDED MODE

If the output voltage is used, the system's open loop transfer function can be expressed as follows:

$$T_{v_{ref}v_{out}} = \frac{\left(\frac{1}{R_L+SL}\right)\times\left(R_f+\frac{1}{SC}\right)}{1+\left(\left(\frac{1}{R_L+SL}\right)\times\left(R_f+\frac{1}{SC}\right)+\left(\frac{1}{R_L+SL}\right)k_{inv}\right)} \quad (14)$$

$$T_{out} = \frac{Z_{out}}{1+T\_v_{ref}\_v_{out}\times T_{Cont}} \quad (15)$$

It should be noted that according to the diagram block model, the value k_{inv} is the inverter parameter or gain is a large value constant. The suggested range is given in [6]. The open loop transfer function considering voltage as output is given in Fig. 13.

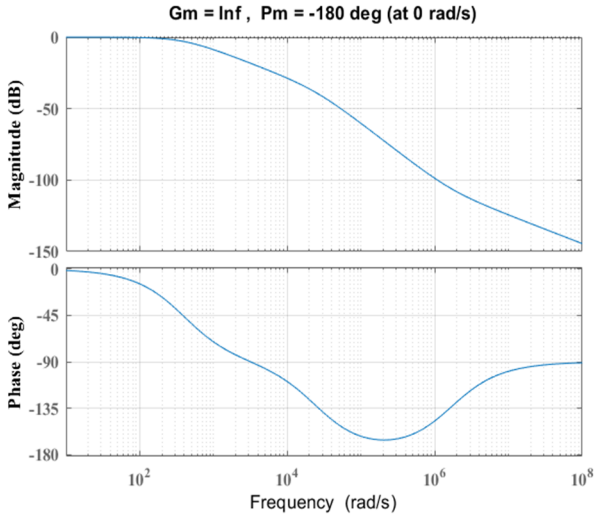

Fig. 13. PHASE AND GAIN MARGIN DIAGRAM WITHOUT VOLTAGE CONTROLLER (MULTI-LOOP MODEL)

Considering the diagram was the open loop of the system, it is clear that the system's response is not, and the phase margin and the system's gain are not in the proper range. As in the previous section, the controller coefficients are determined using the tuning tool to obtain the system response by the following forms.

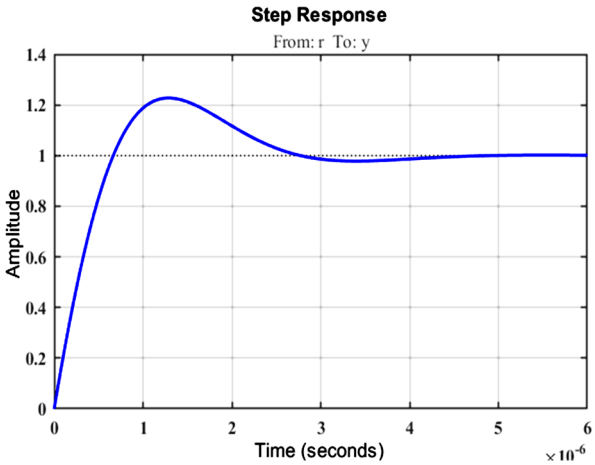

Fig. 14. THE SYSTEM'S STEP RESPONSIVENESS WHEN A VOLTAGE CONTROLLER IS PRESENT

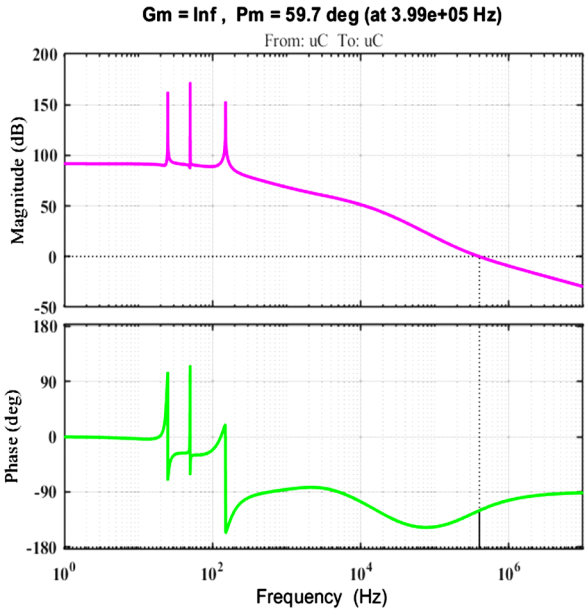

Fig. 15. PHASE AND GAIN MARGIN DIAGRAM IN THE PRESENCE OF VOLTAGE CONTROLLER (MULTI-LOOP MODEL)

Figures 14 and 15 demonstrate how the system response has changed for the better after the controller was designed. Additionally, the system's phase margin falls within the acceptable range.

5.3 Implementation of the Proposed System

Two controllers were created for the simulations above in both the island mode and the grid-connected mode. At first, the system's step response and the bode diagram are designed without any controller scheme. As shown in the figures, the system suffers from poor performance, and the phase margin is undesirable. However, after applying the controllers, the performance has dramatically improved in the voltage and current controller presence. The controller can be programmed to respond to changes in the energy supply and demand, adjusting the output of the green resources and managing energy storage systems within the microgrid. This allows the system to operate stably and sustainably, even when there are fluctuations in the energy supply or demand.

6. CONCLUSION

In this study, the design and control of an AC MG were analyzed and simulated step by step in grid-connected and islanded modes. The block diagram model was modelled in two general modes, and then it was suggested that resonant controllers be used to control voltage and current. Authors have seen that, unlike D.C MGs, one can use them here because they are unsuitable for tracking sinusoidal signals. After designing the controllers and ensuring the

performance of their frequency response using the bode diagram and the system step response, these controllers were used to control the voltage and current in real scenarios. After enabling the controllers, the performance has affectedly enhanced in the voltage and current controllers. The controllers can be programmed to react to fluctuations in the energy source and demand, adjusting the output of the green sources and matching energy storage systems with the microgrid. This allows the proposed system to work in a stable and sustainable mode, even when there are fluctuations in the energy resource or demand.

REFERENCES

[1] N. Mohammed, M. Ali, M. Ciobotaru, and J. Fletcher, 2023.Accurate Control of Virtual Oscillator-Controlled Islanded AC Microgrids. *ElectricPower Systems Research*, 214(12), 10879.

[2] F. Mohammadi, 2020. Integration of AC/DC Microgrids into Power Grids. *Sustainability*, 12(8), P: 1-4.

[3] P. Mansoorhoseini, B.Mozafari, and S. Mohammadi, 2022. Islanded AC/DC Microgrids Supervisory Control: A Novel Stochastic Optimization Approach. Electric Power Systems Research, vol. 209.

[4] D. Espín-Sarzosa, R., Palma-Behnke, and O. Núñez-Mata, 2020. "Energy Management Systems for Microgrids: Main Existing Trends in Centralized Control Architectures", *Energies,* vol.13, (3), P: 547.

[5] Oliveira, T., Caseiro, L., Mendes, A., and Cruz, S., 2020. "Finite Control Set Model Predictive Control for Paralleled Uninterruptible Power Supplies', *Energies*, vol 13, (13), P: 3453.

[6] A. Muhtadi, D. Pandit, 2017, Nguyen, N., and J Mitra, "Distributed Energy Resources Based Microgrid: Review of Architecture", *Control, and Reliability.*

[7] W. Zhou, X.Xu, S. Tan, L. Mao, M. An, and C. Luo, 2020. "Research on Parallel Control Technology of Three-Phase Inverter Based on Multiple Proportional Resonance Controller", *Journal of Physics: Conference Series, (IOP Publishing*.

[8] V. Mortezapour, and H. Lesani, 2018. "Adaptive Primary Droop Control for Islanded Operation of Hybrid AC–DC Mgs", *IET Generation, Transmission & Distribution*, vol. 12, (10), P: 2388-2396.

[9] Z. Afshar, M. Mollayousefi, S.M.T. Bathaee, M.T. Bina, and G.B. Gharehpetian, 2019. 'A Novel Accurate Power Sharing Method Versus Droop Control in Autonomous Microgrids with Critical Loads', *IEEE Access*, vol. 7, P: 89466-89474.

[10] J. Dannehl, M.Liserre, and F.W Fuchs,.2010. 'Filter-Based Active Damping of Voltage Source Converters with LCL Filter', *IEEE Transaction on Industrial Electronics*, vol. 58, (8), P: 3623-3633.

[11] Li, Y.W., 2008. "Control and Resonance Damping of Voltage-Source and Current-Source Converters with LC Filters', *IEEE Transaction on Industrial Electronics,* vol. 56, (5), P: 1511-1521.

[12] Mahlooji, M.H., Mohammadi, H.R., and Rahimi, M., 2018." A Review on Modeling and Control of Grid-Connected Photovoltaic Inverters with Lcl Filter', *Renewable and Sustainable Energy Reviews*, vol.81, P: 563-578.

[13] Shongwe, S. and Hanif, M., 2015. "Comparative Analysis of Different Single-Diode PV Modeling Methods", *IEEE Journal of Photovoltaics*, 5, (3), pp. 938-946.

[14] A. Gargoom, S. Al-Dabbagh, and M. F. Alsulami, 2020."Control strategy of electric vehicle charging stations in a renewable energy-based microgrid," *IEEE Access*, vol. 8, P: 150199-150212.

[15] C. Hu, Z. Zhang, and S. Xie, "Design and optimization of a renewable energy-based microgrid with electric vehicles," Journal of Renewable and Sustainable Energy, vol. 12, no. 5, pp. 053706, 2020.

[16] H. Yang, S. Li, H. Xue, and Y. Liu, "Optimal control of a renewable energy-based microgrid with electric vehicles and energy storage systems," Energies, vol. 14, no. 4, P. 1059, 2021.

[17] X. Li, J. Wang, J. Liu, and C. Jiang, "Design and implementation of a power management system for a renewable energy-based microgrid with electric vehicles," Applied Energy, vol. 255, pp. 113875, 2019.

[18] Y. Li, Y. Zhao, S. Li, X. Wang, and C. Xue, 2019. "Design and control of an electric drive system for a microgrid with renewable energy sources," *Energy Conversion and Management*, vol. 198, P: 111989.

[19] K. A. Khan, A. Atif, M. Khalid, "Hybrid battery-supercapacitor energy storage for enhanced voltage stability in DC microgrids using autonomous control strategy," *Emerging Trends in Energy Storage Systems and Industrial Applications*, *Academic Press,* pp 535-569, 2023.